Analysis of shear failure of surface methane capture boreholes for improving efficient drainage period–A lithology perspective

Hongjie Xu [a, *], Zezhong Fang [a], Shuxun Sang [b, *], Jingfen Yang [a], Huihu Liu [a], Hai Ding [c], Xinzhao Dou [c]

[a] *School of Earth Science and Environmental Engineering, Anhui University of Science and Technology, Huainan, Anhui 232001, China*

[b] *School of Resources and Geoscience, China University of Mining and Technology, Xuzhou, Jiangsu 221008, China*

[c] *Research Institute of Geological Exploration, Anhui Provincial Coalfield Geological Bureau, Hefei 230088, China*

Abstract: The shear failure of surface methane capture borehole (SMCB) is the main cause of shortening life cycle of SMCB but lack of lithological analysis. In order to improve the stability of SMCB and improve efficient drainage period, it is of great significance to investigate the lithology performances for shear failure of SMCB. Based on the direct shear tests and geological method, the results shows that the shear displacement increases as the grain size decreases. Mechanical jump occurs at the lithological boundaries, which is mainly determined by the composition of rock specimens. The cohesion is the mainly possible reason for the step change of shear strength. Lithology with high quartz and low clay may effectively improve shear strength and failure resistance. Boreholes drilled into the weaker siltstone and mudstone sections may potentially experience preferential damage due to the larger shear displacement and shear strength. Protective measures at these sections may improve the stability of the borehole casing. The probing data where it was found that boreholes closure validated the prediction.

Key words: Lithology performance; shear failure; surface methane capture borehole; shear strength

1 Introduction

Drawing surface methane capture borehole (SMCB) around a coal panel is effective method to reduce the methane content of the coal seams [1-3]. SMCB is completed prior to the face retreat and extract the methane in the affected area by coal mining. To date, SMCB has already been extensively used in many coal fields such as Huainan,

Huaibei, Yangquan and Tiefa in China where the permeability of coal reservoirs is rather low, and a great amount of

methane with high concentration [4]. However, when a working face passes near a SMCB, the borehole is likely to

become deformed or even damaged, and the production of the borehole would drop greatly and even emthane

drainage may be suspended (Fig. 1), causing a huge economic loss [5]. For example, 12 of 22 SBCMs in the Huainan

coal field ceased to produce gas as a result of borehole failure, adversely affecting the extraction efficiency [6].
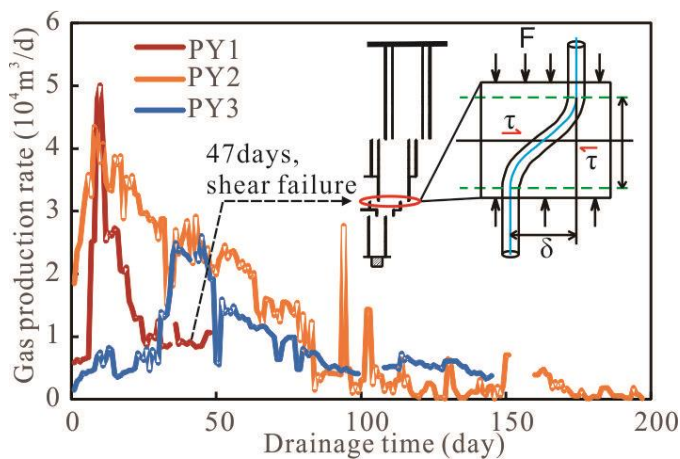

Fig.1. Shear failure of methane capture borehole (τ, horizontal shear stress; δ, shear displacement; d, shear field).

To reduce the probability of borehole failure, previous researches on borehole failure mainly focused on

evaluating drilling design, including the well construction and trajectory, casing material, drilling fluid and typically

assuming that the rock material is isotropic, linear elastic and homogeneous in deformability and strength[7-9], and

extending analyses to anisotropic strength of lithology [10-13] and geostress [14-16].Borehole failure is also

influenced by the chemical-mechanical or physical-mechanical interactions between clay minerals and drilling fluids

as well as groundwater [17, 18], but these effects may be applied to improve drilling methods and maximize the

effectiveness of drilling [19-21].

Despite the recent progress reviewed in the stability of hydrocarbon wells, relatively fewer results are available

to define stability under the influence of overlying strata movement [22]. One reason is that the importance of coalbed

methane reservoirs has only become an important issue relatively recently [23]. However, the estimation of stability

for boreholes piercing mining strata may play an important role in improving the performances of boreholes.

2

Researchers have conducted many studies about coal mining factors [24, 25], geological conditions of overburden [26, 27], failure modes of the borehole casing during mining [28], examination of shear failure through applying shear stress on the well material [26, 29-31] and computational modellings for predicting the stability of well during the extraction life of an active coal panel [5, 28, 32, 33] and the influence of topographic and lithology performance on shear deformation in overburden [22, 34]. Three typical failure modes of the borehole casing were classified, and the tensile and shear failure were thought to be the most common failure modes [28].

Due to the different lithology of the overlying strata, the acting force and shear displacement exerted on the borehole is greatly different. Despite the recent contributions, few analyses exist on the lithology influence on shear failure for SMCB piercing mined coal seams due to experimental difficulties with overlying strata movement and shear displacement in geological conditions. Accordingly, in this paper, direct shear tests of lithological specimens were performed to analyze the change of shear stress on the shear displacement in order to verify the results of the lithology performances for shear failure. Moreover, abundant mechanical parameters are used to justify the results obtained by using the method of direct shear tests and indicate the effect of overlying strata lithology on the possible shear location of the borehole. Therefore, we use this analysis to predict vertical locations where the borehole is prone to fail or more specifically disruption by shear offset with lithology.

2 Experiments and methods

2.1 Specimen preparation

For the shear tests, the rock specimens were taken from a borehole in coal-bearing strata in Huainan mining area, Anhui Province, China. In order to understand the shear strength of lithological geology, the utilized specimens include coarse sandstone, medium sandstone, fine sandstone, siltstone and mudstone, which are the most representative and natural lithology types without obvious macroscopic cracks. In addition, it is difficult to collect core samples about structural plane to define their truly mechanical parameters through experiments. Thus, only 25

specimens in 5 groups were performed using the direct shearing machine.

These core samples were properly packed, and then were sent to the laboratory immediately after classification and packing. During the sample preparation process, core samples with a diameter of 50 mm were cut at a ratio of 1:1 in the aspect ratio in accordance with the GB/T 50266-2013. After cutting, each surface of all samples was ground to ensure a flat surface. Fig 2 presents parts of specimens before and after direct shear tests, and apparent shear failure planes occurred in the middle of the specimens after completed tests. The sample number shown in Table 1 is provided as follows: the first digit indicates the rock lithology, and the second digit indicates the sequential number of the specimens in each group.
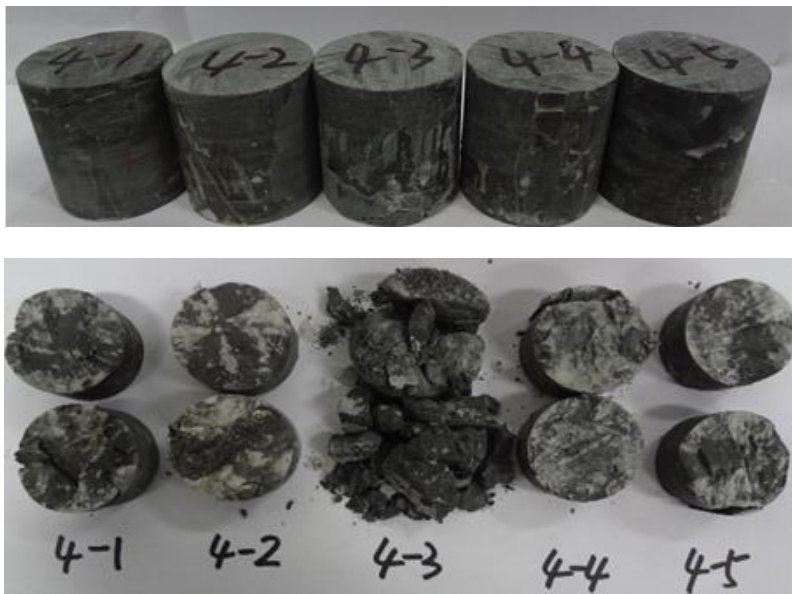

Fig. 2 Parts of specimens before and after direct shear tests.

2.2 Tests apparatus

In this study, the direct shear tests on core specimens were performed using a multi-functional testing machine and manufactured in the State Key Laboratory of Geohazard Prevention and Geoenvironment Protection of Chengdu University of Technology, China. Despite it would be more accurate to measure shear strength of soil using tri-axial apparatus with considering the applying confinements in the field, the direct shear apparatus was considered adequate to respond to the desired results of shear behavior about the lithological aspects.

Fig.3 shows the direct shear test apparatus to examine failure behavior of lithology instead of applying shear stress on the well material. Two hydraulic jacks controlled by pressure oil pumps are fixed in the top and right side of the stiff loading frame, respectively. The maximum loads provided by the two hydraulic jacks are 294 kN and 490 kN with oil cylinder maximum trip of 60 mm, respectively. The device has lower and upper shear boxes equipped with one row of ball bearings. The lower shear box is fixed, and the upper shear box can produce dislocation. The upper and lower shear rings are placed in the inner hole of the shear box which is consisted of four surface ground steel. Appropriate size and shape of shear rings are designed (Fig.3d).

Measured data from 8 channels can be collected simultaneously. The sensors and the other instruments were calibrated as required before each sample was tested. The range of pressure sensor and displacement is 0-40 MPa and 0-50 mm with a resolution of 0.01 MPa and 0.01 mm, respectively.
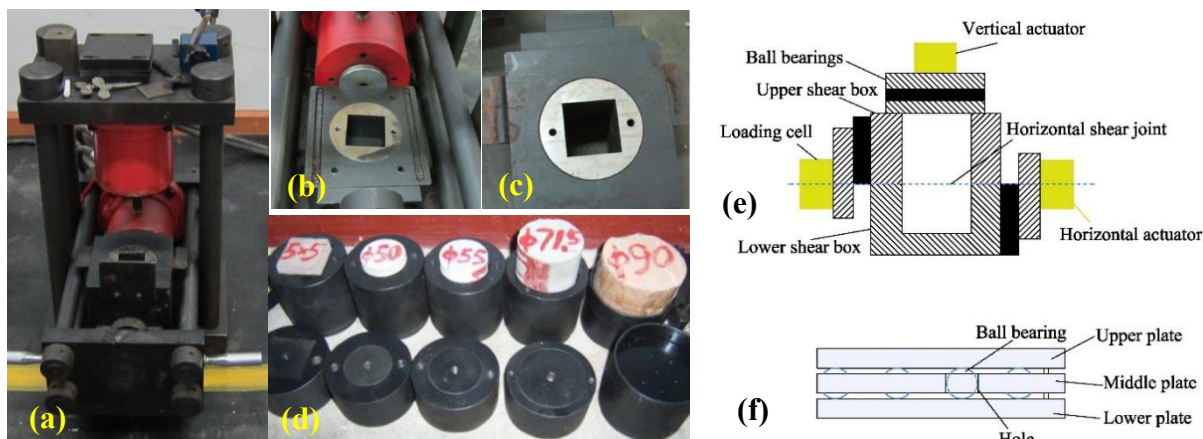

Fig.3 Test system of specimen in direct shear test (a, Direct shear test apparatus; b, Lower shear box; c, Upper shear box; d, shear rings; e, Experimental device; f, Ball bearings).

2.3 Test procedure

In this study, the testing procedure followed the Chinese standard GB/T50266-2013. Five specimens in each group were applied with normal stress of 2, 3, 4, 5 and 6 MPa, respectively. The usual test procedure adopted for conducted direct shear tests calls for a constant normal load (CNL) to be applied with the horizontal load being gradually increased until sliding takes place. The test process includes two main steps: (1) load the initial normal

stress to the desired value at a loading rate of 0.08 kN/s; (2) load the shear stress until the failure of specimen occurs with a constant shear speed of 0.2 mm/min. In the process of direct shear, the rock would dilate when it was destroyed, then the tested data of the normal stress may be inconsistent with the set normal stress. In these tests, the shear displacements and loads in the normal and shear directions were recorded automatically throughout the test.

2.4 Estimating method of shear strength

The volume of the standard specimen was calculated by measuring the cross-sectional area and height of the sample, then the mass of the specimen was weighed. The density of the rock block can be obtained by using the relationship between volume and quality. The normal stress and shear stress can be calculated by the following formula respectively:

$$\sigma = \frac{(I_\sigma - I_{\sigma 0}) \times S_\upsilon + G}{S_j} \qquad (1)$$

$$\tau = \frac{(I_\tau - I_{\tau 0}) \times S_h}{S_j} \qquad (2)$$

Where, σ is the normal stress, MPa; I_σ, set pressure value of normal cylinder, MPa; $I_{\sigma 0}$, initial normal pressure applied on the sample, MPa; $I_{\sigma 0}$, piston area of normal cylinder, m²; G, total weight of iron and ball bearing, MN; S_j , shear area of the sample, m²; τ, shearing strength, MPa; I_τ, maximum value of shear load, MPa; S_h ,piston area of shear cylinder, m².

One many now use the Mohr-Coulomb criterion (Eq. (3)) to express the peak and residual shear strengths versus the normal stress as shown in Fig. 4 according to the obtained cohesion and friction angle:

$$\tau = c + \sigma_n tan\varphi \qquad (3)$$

whereτ, c, σ_n and φ are shear strength, cohesion, normal stress and friction angle, respectively [35].

The applied experimental data used in this study, such as Poisson's ratio, elasticity modulus, compressive strength, tensile strength, angle of internal friction and cohesion were collected from the results of tests and measurements of core samples. Microscopic examinations were used for petrographic analysis based on the

polarizing microscope, scanning electron microscope equipped with a ZEISS SIGMA system.

3 Results and discussions

3.1 Shear failure characteristics

Peak and residual tests were carried out for each sample according to the test program. Tests in residual state were conducted to estimate the residual shear strength parameters. Results of all direct shear tests on rock specimens are summarized in Table 1. Although the experiments were carried out carefully according to specific methods, some tested parameters were of poor quality and omitted for the heterogeneity of rocks, such as 1-2, 3-3, 3-4 and 5-4 specimens in Table 1.

Table 1 Direct shear testing results for rock specimens.

Lithology	Group ID	Sample ID	Bulk density (g/cm³)	Normal stress (MPa)	Peak shear stress (MPa)	Yield shear stress (MPa)	Residual shear stress (MPa)
Coarse sandstone	1	1-1	2.58	5.11	23.4	18.72	4.86
		1-2		2.3	19.74	15.79	5.89*
		1-3		3.07	18.63	14.9	4.09
		1-4		4.09	21.1	16.88	5.7
		1-5		5.92	25.76	20.61	6.68
Medium sandstone	2	2-1	2.55	2.05	14.15	11.32	3.86
		2-2		3	16.97	13.58	3.56
		2-3		4.15	15.48	12.38	4.39
		2-4		5.14	17.99	14.39	6.5
		2-5		6.49	21.89	17.52	8.52
Fine sandstone	3	3-1	2.65	2.07	16.79	13.43	9.32
		3-2		3.25	19.73	15.78	9.17
		3-3		4.35	21.18	16.95	7.11*
		3-4		5.37	21.44	17.15	5.71*
		3-5		6.16	27.25	21.8	15.59
Siltstone	4	4-1	2.65	2.32	10.24	8.19	4.62
		4-2		3.14	8.11	6.48	6.58
		4-3		1.23	8.75	7	5.49
		4-4		5.06	18.56	14.85	8.39
		4-5		6.23	19.15	15.32	10.86
Mudstone	5	5-1	2.65	2.12	6.46	5.16	4.67
		5-2		3.35	7.29	5.83	5.68
		5-3		5.05	7.73	6.18	5.92
		5-4		5.2	26.71*	21.37	9.09
		5-5		6.19	11.09	8.87	8.11

Note: *, invalid data.

For each test specimen, graphs of shear stress versus shear displacement were plotted. As illustrated in Fig. 4, all curves have similar trend that the shear stress level dropped to a residual state after the peak strength. The shear displacement of most specimens increases with an increasing shear stress, showing a large slope. After the shear stress reaches the peak strength, the shear stress decreases dramatically as the shear displacement increases. However, some specimens show a significant increase of shear displacement with slowly increased shear stress at the initial stage, such as 3-2 and 4-3 specimens.

The shear curve increases significantly after the shear displacement reached a certain value (about less than 0.5 mm to 1.0 mm) until the peak stress is reached, and a change of shear stress occurs at the peak. The slope of the curve changes from positive to negative with a noticeable trend, indicating obvious brittle failure characteristic of the lithological specimens with a release of cohesion. As the displacement continues, the shear stress falls to a certain residual value that then remains constant, even for larger shear displacements. The residual stress varies greatly, generally about 21%-78% of the peak stress. It indicates that the specimen has been completely destroyed, but still has a certain load capacity under external force.

In addition, five different normal stress levels were considered to study the effect of normal stress on the shear behavior of rock samples. The peak shear strengths of five lithology groups follows an increase with the increasing of normal stress. According to the data obtained from 5 groups of direct shear test results, the relationship between the peak shear strength and normal stress expressed by the Mohr-Coulomb criterion, Eq. (3) are plotted as shown in Fig. 5.
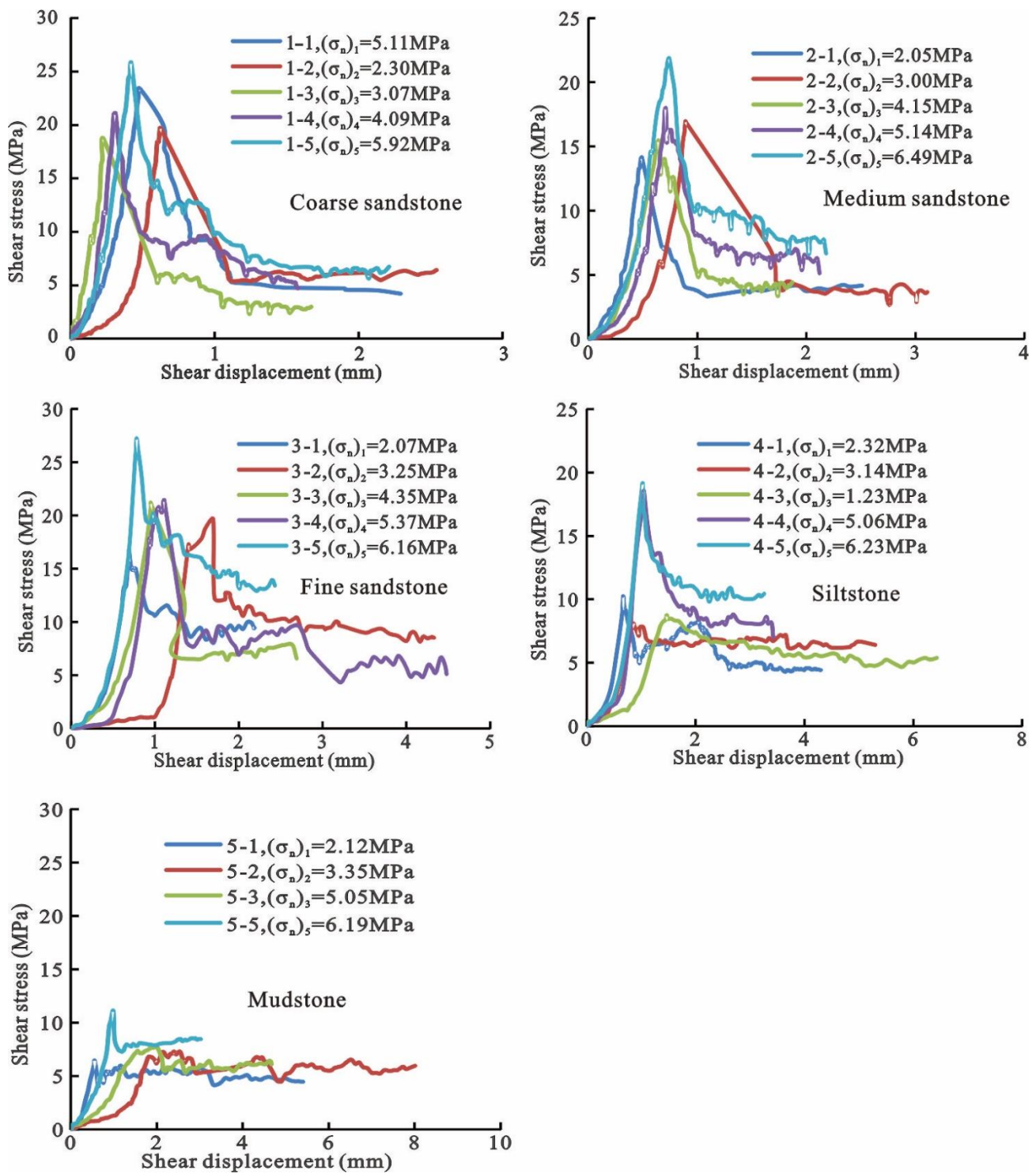
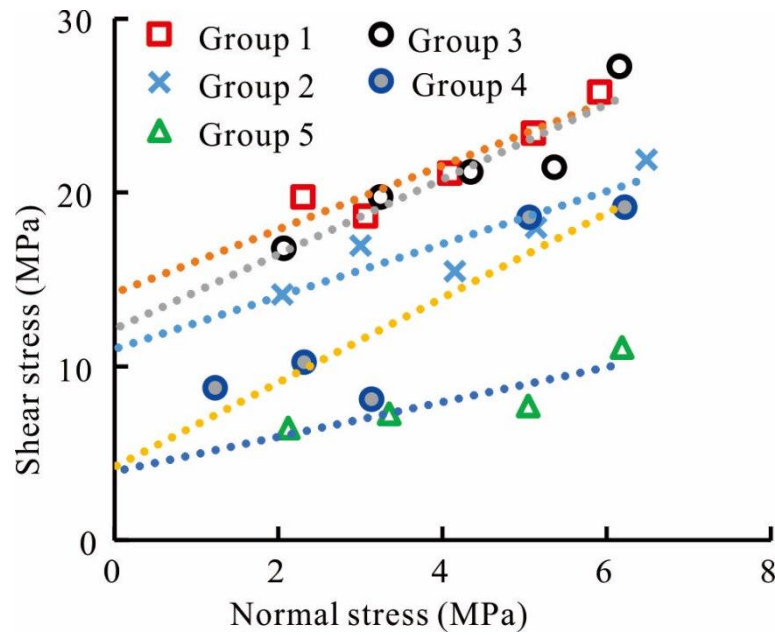Fig. 4 Shear stress-shear displacement curves of rock specimens under different normal forces.

Fig. 5 Shear strength curve of the specimens (Group 1, $\tau=14.23+1.83\sigma$, $R^2=0.88$; Group 2, $\tau=11.00+1.51\sigma$, $R^2=0.80$; Group 3, $\tau=12.17+2.15\sigma$, $R^2=0.85$; Group 4, $\tau=4.22+2.43\sigma$, $R^2=0.82$; Group 5, $\tau=4.01+1.05\sigma$, $R^2=0.58$).

3.2 Influence of lithology on mechanical parameters

Fig. 6 shows that the residual strength of the specimens with different lithology was substantially smaller than

the peak strength. With the lithology changes from coarse sandstone to mudstone (the grain size changes from coarse

to fine), the magnitude of peak shear stress strength and yield shear strength takes on reducing trends, which is most

obvious from siltstone to mudstone as shown in Fig. 6.

Coarse-grained lithology has a larger stress drop than fine-grained lithology. Generally, the process of stress

drop is essentially a process of gradual penetration of fracture surface. However, as shown in Fig. 5, there is no

significant change in the friction angle of all specimens, indicating that the crucial change of peak strength and yield

strength is mainly caused by cohesion. The change of stress drop values with lithology indicates that the cohesion

changes from large to small when the lithological grains change from coarse to fine. With the change of lithology,

the more the clay content is, the more the strength is reduced. The drop value has a certain relationship with the

cohesive force [36]. Compared with lithology composed of fine grain size, lithology with coarse grain has smaller

residual shear strength but larger peak shear strength.
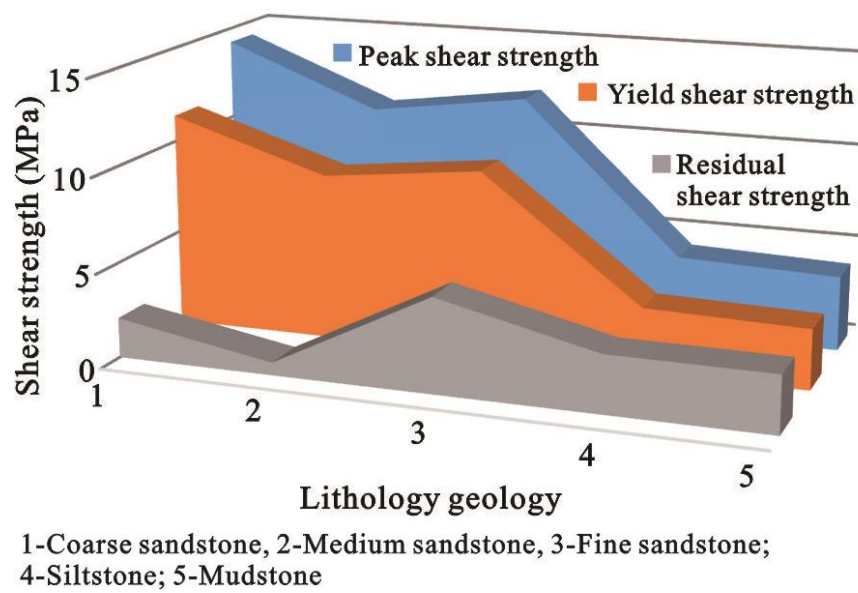
Fig. 6 Variation of shear strength showing influence of lithology geology.

By comparing the relationship between peak shear stress and shear displacement under different normal stresses (Fig. 7), it can be found that the peak shear stress generally shows a decreasing trend corresponding to the increasing shear displacement with the decrease of clastic grain size of rock composition under a given similar normal stress. When the normal stresses are 2, 3, 5, and 6 MPa, the change of the shear stress vs. lithology curves indicates that the peak shear strengths of the specimens follows an decrease with decreasing grain size of changing lithology. In addition, the shear displacements increases gradually from coarse sandstone to mudstone. Thus, the variation of the shear strength and displacement with different lithology specimens indicates that grain size of different lithology has an important effect on shear strength. The smaller the grain size of lithology, the smaller the peak shear stress and the larger the shear displacement. Namely, the rock with small grain composition tends to give priority to shear failure with large shear displacement, such as mudstone or siltstone.
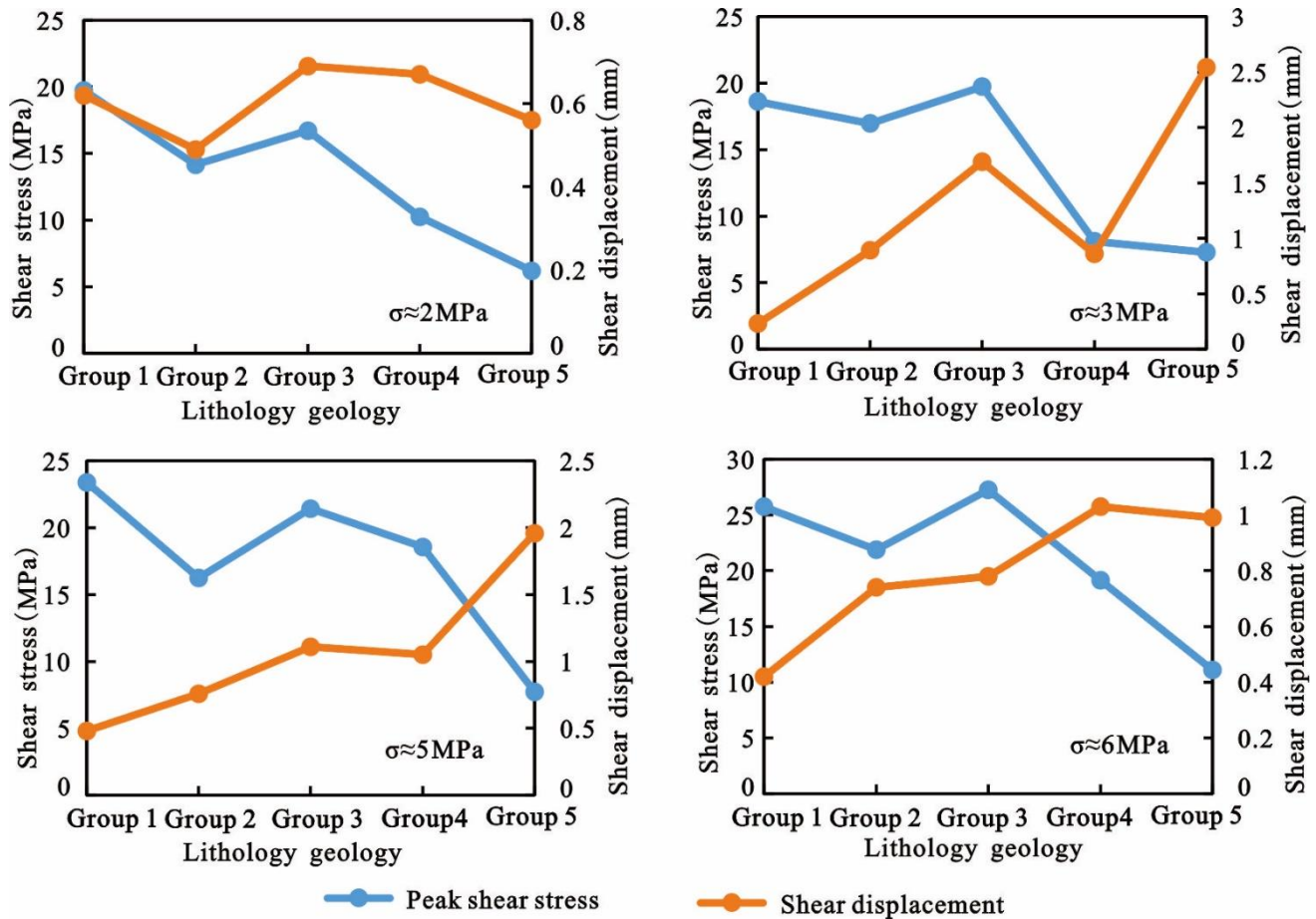
.

Fig.7 Variations of the peak shear stress and shear displacement vs. lithology geology with normal stresses of 2, 3, 5 and 6 MPa.

In order to better understand the mechanical properties of different lithology geology, about 330 tested mechanics parameters of coal-bearing rock samples were collected from Huainan mining area, China. Fig. 8 depicts the main mechanical parameters of these lithology samples. The lithology geology changing from medium sandstone to fine sandstone, siltstone and mudstone, namely, the decrease of the grain diameter, shows a step drop of mechanical parameters when the lithology changes, which behaves as grain diameter softening [37]. As data shown in Fig.8, The mechanical parameters of rock samples, such as compressive strength, tensile strength, cohesion and elastic modulus have two obvious changes on the boundary of medium and fine sandstone, fine sandstone and mudstone. It is evident that medium and fine sandstone has the same mechanical parameters (Fig.8), which is not expected due to the change in lithology. This may be related to the fact that the cement of medium and fine sandstones is mainly quartz with grain-supported texture. The mechanical parameters of medium sandstone are relatively discrete (Fig.8), which

indicates that the increasing of quartz may be limited to improve the mechanical strength of rocks in the study area.

If these samples are classified as medium-fine sandstone, siltstone and mudstone, the average values of some

mechanical parameters of them are summarized in Table 2. Taking medium-fine sandstone as the datum, the cohesion

of siltstone and mudstone decreases by 44% and 67%, the elastic modulus by 47% and 70%, the compressive strength

by 42% and 65%, the tensile strength by 51% and 69%, and the Poisson's ratio increases by 9% and 12%, respectively.

However, the poisson ratio goes up step by step and the friction angle has no obvious change.
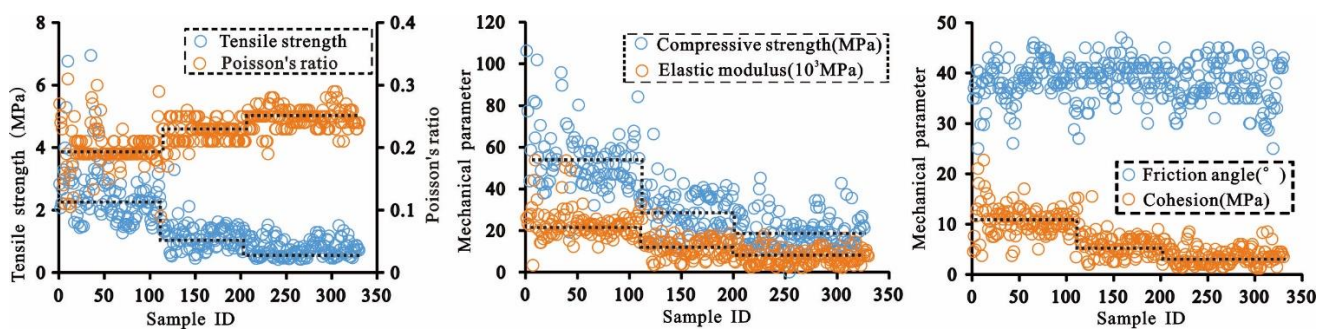

Fig. 8 Variation of some mechanical parameters from collected 330 samples (ID 1-34, medium sandstone; ID 35-107, fine sandstone; ID 108-206, siltstone; ID 207-330, mudstone).

Table 2 Average values of mechanical parameters obtained from collected 330 samples.

Lithology geology	Friction angle(°)	Cohesion(MPa)	Elastic modulus （10³MPa）	Poisson's ratio	Compressive strength （MPa）	Tensile strength （MPa）
Medium--fine sandstone （107）	38.6	10.7	23.4	0.2	54	2.52
Siltstone （99）	39.1	6	12.5	0.22	31.1	1.23
Mudstone （124）	37.7	3.5	7.1	0.25	18.9	0.77

3.3 lithology performances for shear failure of SMCBs

Based on the statistical results shown in Fig. 8 and Table 2, the siltstone and mudstone composed of fine particles

have generally lower shear strength than the medium-fine sandstone (Fig. 9a). There is no obvious change in the

internal friction angle of different lithological samples, suggesting that the shear strength and shear displacement are

mainly determined by cohesion of them. When the grain size of rock mineral composition increases to the sand-size,

the lithological rock has high mechanical strength because of their mineral composition of single-crystal quartz (Fig.
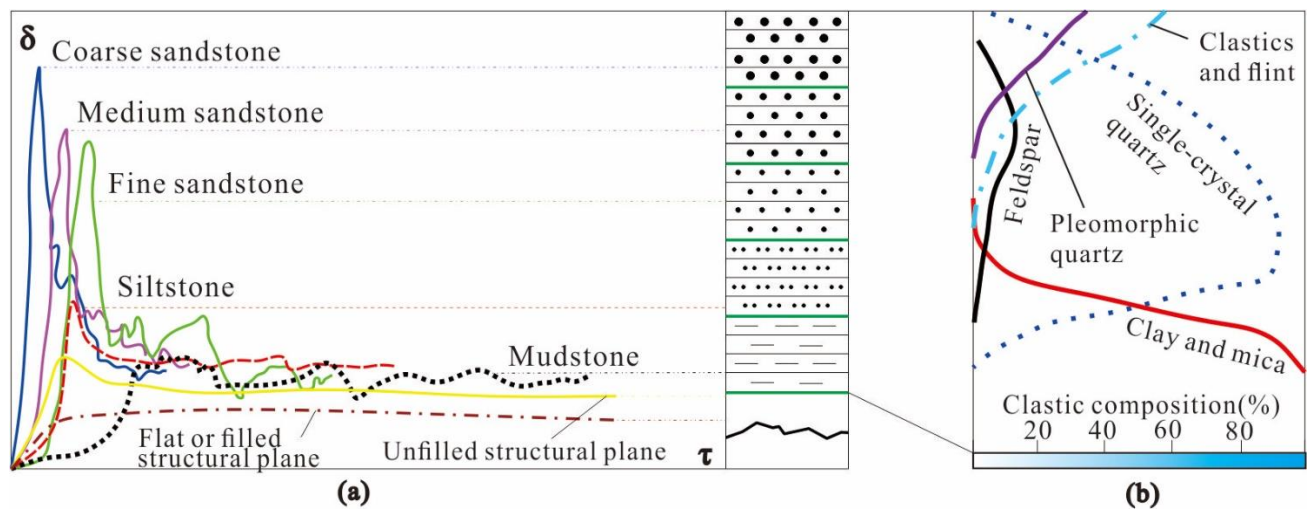
9b).

Fig. 9 Lithology performances for mechanical parameters caused by mineral compositions (b is modified from Meng et al., 2000).

In addition, some factors such as cementation also play an important role in the mechanical properties of rock shear. The observed particle-supported sandstone sample generally shows high mechanical strength with siliceous and ferruginous cementation (Fig.10a). However, the siltstone and mudstone, mainly composed of clay and sliced mica, have low mechanical strength for their developed inter-fracture and weak stiffness. Compared with sandstone, mudstone has high clay content with poor argillaceous cementation (Fig.10b). The clay minerals by X-ray diffraction analysis is 59.0%, and the proportion of kaolinite and the mixed layer of illite and smectite in clay minerals can reach 40% or more [38]. As shown in Fig. 10c, a large amount of flaky clay minerals in the mudstone samples can be observed by scanning electron microscopy. The flaky texture with weak interlayer mechanics interaction provides the possibility of microscopic shear and slippage.

Thus, the mineral composition and cement of mudstone can significantly weaken its mechanical strength. To sum up, with the decrease of the grain diameter of lithology rocks (lithology geology from sandstone to mudstone), decreasing quartz and increasing clay minerals are the important factors for the decrease of shear strength and cohesion, which further leads to weakening of shear strength of lithology rock. Therefore, the lithology performance with varying shear mechanical parameters has significantly effect on the sequence and location of potential shear
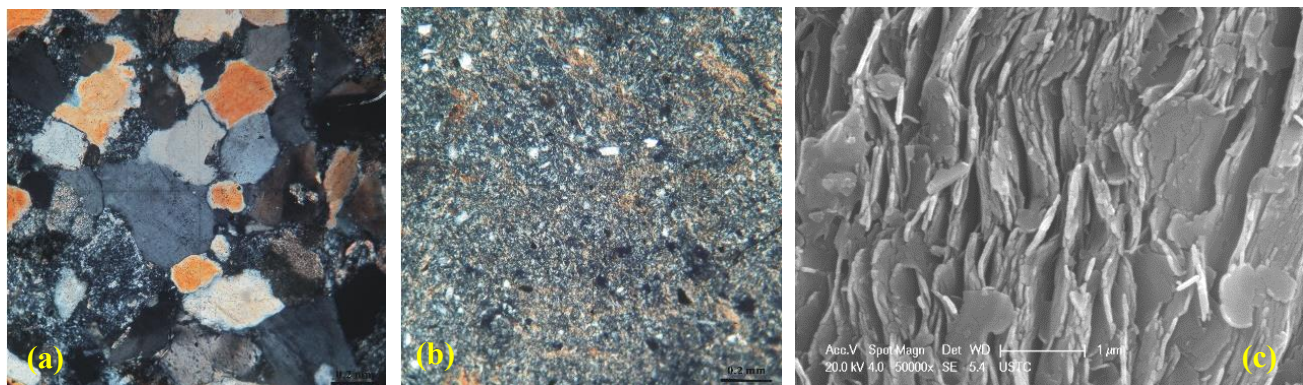
failure for SMCB in drilled strata.

Fig. 10 Thin-sections and SEM photomicrographs showing diagenetic minerals of sandstones and mudstones in coal-bearing strata in

Huainan mining area. (a) Sandstone displays the wide array of medium-grained quartz with approximately 80% of the rock composition.

The majority of framework grains showing porous cementation. Minor amounts of siderite cements quartz grains. Detrital silty mudstone

grain is present in small quantities as a matrix within the grain-supported sand. Cross-polarized light. (b) Silt-bearing mudstone showing

a majority grains are silt-grained and clay, about 10% and 90%, respectively. The detrital composition is mainly quartz with a small

amount of feldspar. Minor amounts of the detrital grain size is 0.08 mm. Cross-polarized light. (c) SEM photomicrograph showing

relatively textural, flaky clay minerals of mudstone.

Moreover, there may be many failures for methane capture borehole around the panel because of mining. The

lithology performance and possible optimal location of shear failure is analyzed, but other factors such as geological,

structural plane and dip angle may affect the lithology performance for shear failure. The cohesion of structural plane

is generally 0.005-1.0 [39], which shows significant difference compared to rocks. In a conventional way, the thick

interlayer will decrease the shear strength of structural plane, and increased filling particles implies decreased shear

strength. As for the mudstone interlayer, the increase of water content will also cause an obvious decrease of the

cohesion and friction coefficient of the structure surface [40].

The conclusions are reasonable and coincide with the engineering practice. Fig.11 displays stratigraphic sections

of the overlying strata in some damaged boreholes induced by shear failure, and these sections are mainly mudstone,

siltstone and lithological boundaries. Compared with the failure of rock masses of different lithology geology, the driving force required for generating slippage and instability along the structural surface is smaller, and the shear failure caused by structural plane is more preferential.
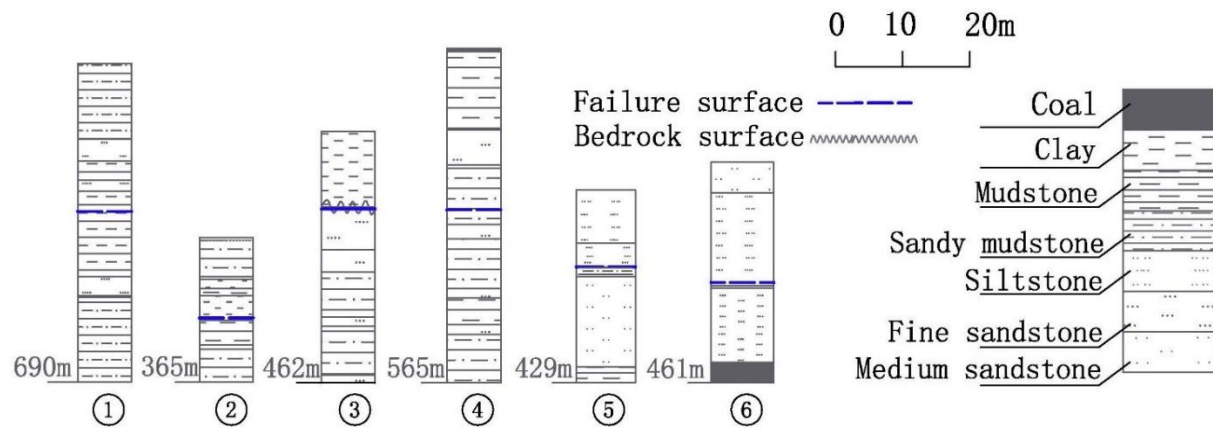

Fig. 11 Stratigraphic sections of the strata in some damaged boreholes in the Huainan mining area (Modified from [41]).

However, the shear failure of casing is affected by overlying strata movement, mining engineering and geological conditions, etc. Tested mechanical properties are related to physical properties of rock mass such as water content and porosity, as well as the processing and loading of specimens. The lithology performance for shear failure of SMCB is only obtained from the tests carried out with few specimens in this paper, and the conclusions still need to be further studied.

4 Conclusions

In this study, the direct shear test under constant normal condition was carried to investigate the shear responses of lithology specimens. The effects of the displacement and shear strength on the lithology performance and shear failure possibility of specimens are highlighted. Several conclusions are drawn as follows:

(1) Lithology specimens show that the shear strength linearly increases with the increase of initial normal stress. Nearly all specimens of shear stress show the tendency to increase first and then decrease as the shear displacement increases, indicating obvious brittle failure characteristics.

(2) With the lithology changes from coarse sandstone to mudstone (the grain size changes from coarse to fine),

the shear stress has obvious trend of decreasing with significant shear displacement. Therefore, in the section of siltstone, mudstone and structural plane with weak mechanical properties, the casing is more likely to undergo shear displacement to shear failure. Protective measures at these sections may improve the stability of the borehole casing.

(3) The jump of the rock mechanics properties at the lithological boundaries is in response to the changes of lithological grain size, which is mainly determined by the composition of rock specimens. The cohesion is the main reason for the step change of shear strength. The lithology sections which have low content of quartz and high content of clay, may be have poor shear strength and failure resistance, and they are the highest possible failure sections of the borehole from the surface to the coal seam.

Acknowledgements

References

[1] Feng G, Hu S, Li Z, Jiang H, Zhang Y, Xu G, et al. Distribution of methane enrichment zone in abandoned coal mine and methane drainage by surface vertical boreholes: A case study from China. Journal of Natural Gas Science and Engineering. 2016;34:767-78.

[2] Karacan CÖ. Analysis of gob gas venthole production performances for strata gas control in longwall mining. Int J Rock Mech Min Sci. 2015;79:9-18.

[3] Yuan L. Control of coal and gas outbursts in Huainan mines in China: A review. Journal of Rock Mechanics and Geotechnical Engineering. 2016;8:559-67.

[4] Sang S, Xu H, Fang L, Li G, Huang H. Stress relief coalbed methane drainage by surface vertical wells in China. International Journal of Coal Geology. 2010;82:196-203.

[5] Liu Y, Zhou F, Geng X, Chang L, Kang J, Cui G, et al. A prediction model and numerical simulation of the location of the longwall face during the highest possible failure period of gob gas ventholes. Journal of Natural Gas Science

and Engineering. 2017;37:178-91.

[6] Huang H, Sang S, Fang L, Li G, Xu H, Ren B. Optimum location of surface wells for remote pressure relief coalbed methane drainage in mining areas. Mining Science and Technology (China). 2010;20:230-7.

[7] Bradely WB. Failure on inclined boreholes. Journal of Energy Resources Technology. 1979;102:232-9.

[8] Santarelli FJ, Brown ET, Maury V. Analysis of Borehole stresses using pressure-dependent, linear elasticity. Int J Rock Mech Min Sci. 1986;23:445-9.

[9] Kiran R, Teodoriu C, Dadmohammadi Y, Nygaard R, Wood D, Mokhtari M, et al. Identification and evaluation of well integrity and causes of failure of well integrity barriers (A review). Journal of Natural Gas Science and Engineering. 2017;45:511-26.

[10] Périé P-J. Laboratory investigation of rock fracture around boreholes: University of California, Berkeley; 1990.

[11] Ajalloeian R, Lashkaripour GR. Strength anisotropies in mudrocks. Bulletin of Engineering Geology and the Environment. 2000;59:195-9.

[12] Lee H, Ong SH, Azeemuddin M, Goodman H. A wellbore stability model for formations with anisotropic rock strengths. Journal of Petroleum Science and Engineering. 2012;96-97:109-19.

[13] Tien YM, Kuo MC, Juang CH. An experimental investigation of the failure mechanism of simulated transversely isotropic rocks. Int J Rock Mech Min Sci. 2006;43:1163-81.

[14] Addis MA, Wu B. The role of the intermediate principal stress in wellbore stability studies: Evidence from hollow cylinder tests. International Journal of Rock Mechanics and Mining Science. 1993;30:1027-30.

[15] Song I. Borehole breakouts and core disking in westerly granite: mechanisms of formation and relationship in situ stress: University of Wisconsin--Madison; 1998.

[16] Yan W, Zou L, Li H, Deng J, Ge H, Wang H. Investigation of casing deformation during hydraulic fracturing in high geo-stress shale gas play. Journal of Petroleum Science and Engineering. 2017;150:22-9.

[17] Haimson BC, Song IJIJoRM. Laboratory study of borehole breakouts in Cordova Cream: a case of shear failure mechanism. International Journal of Rock Mechanics Mining Sciences. 1993;30:1047-56.

[18] Zeynali ME. Mechanical and physico-chemical aspects of wellbore stability during drilling operations. Journal of Petroleum Science and Engineering. 2012;82-83:120-4.

[19] Supon SB, Adewumi MA. An Experimental Study of the Annulus Pressure Drop in a Simulated Air-Drilling Operation. SPE-19334-PA. 1991;6:74-80.

[20] Bennion DB, Thomas FB, Bietz RF. Low Permeability Gas Reservoirs: Problems, Opportunities and Solutions for Drilling, Completion, Stimulation and Production. SPE Gas Technology Symposium. Calgary, Alberta, Canada:

Society of Petroleum Engineers; 1996. p. 15.

[21] Clancey BM, Khemakhem ASD, Bene TF, Schmidt MH. Design, Construction And Optimization Of Big-Bore Gas Wells In A Giant Offshore Field. SPE/IADC Drilling Conference. Amsterdam, The Netherlands: Society of Petroleum Engineers; 2007. p. 9.

[22] Liang S, Elsworth D, Li X, Yang D. Topographic influence on stability for gas wells penetrating longwall mining areas. International Journal of Coal Geology. 2014;132:23-36.

[23] Wang Y, Watson R, Rostami J, Wang JY, Limbruner M, He Z. Study of borehole stability of Marcellus shale wells in longwall mining areas. Journal of Petroleum Exploration and Production Technology. 2014;4:59-71.

[24] Xu H, Sang S, Fang L, Huang H, Ren B. Failure characteristics of surface vertical wells for relieved coal gas and their influencing factors in Huainan mining area. Mining Science and Technology (China). 2011;21:83-8.

[25] Zhang J. Analysis on the main control factors of deformation and failure for surface gas extraction drilling. Safety in Coal Mines. 2012;43:149-53.

[26] Peng S, Fu J, Zhang J. Borehole casing failure analysis in unconsolidated formations: A case study. Journal of Petroleum Science and Engineering. 2007;59:226-38.

[27] Diwan P, B P Kumar Pandey D, Dharmendra G, Ayyappan S. A fresh look at wellbore stability analysis to sustainable development of natural resources: Issues and opportunities. International Journal of Science Technology & Management. 2011;2:55-63.

[28] Chen J, Wang T, Zhou Y, Zhu Y, Wang X. Failure modes of the surface venthole casing during longwall coal extraction: A case study. International Journal of Coal Geology. 2012;90-91:135-48.

[29] Sun H, Zhang Y. Analysis on Deformation and Fracturing Factors of Surface Gas Drainage Holes and Preventive Measures. Mining Safety & Environmental Protection. 2010;37:79-81.

[30] Li RF, Liang YP, Ou C, Mou JS. Analysis on stability factors of surface boreholes for gob gas drainage and Extraction2008.

[31] Davies RJ, Almond S, Ward RS, Jackson RB, Adams C, Worrall F, et al. Oil and gas wells and their integrity: Implications for shale and unconventional resource exploitation. Mar Pet Geol. 2014;56:239-54.

[32] Whittles D, Lowndes I, Kingman S, Yates C, Jobling S. The stability of methane capture boreholes around a long wall coal panel. International Journal of Coal Geology. 2007;71:313-28.

[33] Liu C, Zhou F, Yang K, Xiao X, Liu Y. Failure analysis of borehole liners in soft coal seam for gas drainage. Eng Failure Anal. 2014;42:274-83.

[34] Xu H, Sang SX, Han JZ, Huang HZ, Cheng ZZ, Ren B. Relationship between rock mass structure and stability

of surface well for released coal gas. Journal of Mining & Safety Engineering. 2011;28:90-5.

[35] Hoek E. Practical rock engineering. Canada: North Vancouver; 2000.

[36] Zhang G, Yinping LI, Yang C, Wang L, Yang C. Discussion on relationship between post-peak curves and shear strength parameters of rock subjected to direct shear tests. Chinese Journal of Rock Mechanics and Engineering. 2012;31:2981-8.

[37] Meng Z, Peng S, Qu H. Relationship between composition and texture of sedimentary rock and its mechanical properties in the roof and floor. Chinese Journal of Rock Mechanics and Engineering. 2000;19:136-9.

[38] Xu HJ, Hu BL, Liu HH, Zheng JB, Zhang WY, Zheng KG. Reservoir characteristics and its physical origin of shale gas in coal measure in the Lower Permian Shanxi Formation in Huainan coal field. Natural Gas Geoscience. 2015;26:1200-10.

[39] Brady BHG. Rock Mechanics for underground mining Third edition. In: Brown ET, editor. Springer Netherlands: Dordrecht; 2006.

[40] Papaliangas T, Hencher SR, Lumsden AC, Manolopoulou S. The effect of frictional fill thickness on the shear strength of rock discontinuities. International Journal of Rock Mechanics and Mining Sciences & Geomechanics. 1993;30:81-91.

[41] Xu HJ, Sang SS, Huan HZ, Liu HH, Wu J, Ren B, Han JZ. Geological mechanism of failure surface vertical boreholes for relieved methane drainage in coal mining area. Hydrogeology & Engineering Geology. 2014; 41: 122-7.